Gravitational waves from colliding black holes

Chris Pedersen

April 9, 2017

Abstract

B B B B B Binnnaryyyy..

1 Introduction

1.1 A Brief History

The first[1] and subsequent[2] observations of gravitational waves (GWs) came around the centenary of Einstein's theoretical prediction of their existence[3][4]. Einstein noticed that a solution to the linearised approximations of his field equations took the form of a wave equation[5], and that the source of these waves would be an asymmetric, massive, rotating system, such as a binary star system. As the amplitude of the waves was predicted to be so incredibly weak, with strain amplitudes on the order of 10^{-24}, at the time there was no hope of ever actually detecting them, and Einstein even questioned whether they were physically real at all[6]. Observations of the Hulse-Taylor pulsar (PSR 1913+16)[7] showed that the energy loss of the binary agreed perfectly with the rate predicted by gravitational wave emission, leading to the award of the 1993 Nobel Prize in Physics, but it was not until the construction of the Laser-Interferometric Gravitational wave Observatory (LIGO) that direct detection of gravitational waves became possible - a truly remarkable feat of science and engineering involving the most precise measurements ever made by several orders of magnitude.

Now that the existence of gravitational waves has been confirmed and their detection is possible we enter a new era of astronomy, and it is difficult to overstate the wealth of science that is now attainable in the coming decades. Gravitational waves can be used to study astrophysical phenomena that cannot be observed using electromagnetic radiation, such as binary black hole (BBH) systems where two inspiralling black holes merge into one, as well as being used in conjunction with electromagnetic observations in 'multi-messenger' astronomy where events such as supernovae and gamma ray bursts are thought to release both gravitational and electromagnetic radiation which can be studied in conjunction with one another[8][9]. In addition GWs can be used to conduct the closest tests of general relativity (GR) to date, (CITE CAL's) as well as to further inform the ongoing development of quantum gravity models[10]. Currently the LIGO network consists of two detectors, one in Hanford WA (H1), one in Livingston LA (L1), however there are three detectors that will be added to the network in the coming years, with VIRGO (V1) in Italy due to come online by the end of 2017, and with LIGO India and KAGRA joining later. In addition to this, there are also proposals underway for a space-based gravitational wave observatory, the Laster Interferometric Space Antenna (LISA)[11] which would be able to explore a different frequency-range and therefore study a range of different astrophysical objects to earth-based detectors.

This project focuses on studying the merging of a binary system, known as a compact binary coalesence (CBC). This term includes the merging of binary neutron star systems and neutron star-black hole systems, but in this work we focus on the merging of BBHs, where we do not consider the internal structure of the compact binary objects unlike in the case of systems involving neutron stars. We focus on parameter estimation of BBH mergers, with a specific emphasis on inferring the

spin parameters of the component BHs in systems where the spins are misaligned, and how they can be determined though careful analysis of LIGO data.

The work is structured as follows; first we present an overview of gravitational wave theory and the LIGO detectors. We then discuss the process of parameter estimation and the mathematical and computational models that are used. Next we consider the case of systems with misaligned spins where relativistic precession is manifested, and consider the specific set of challenges this raises for signal analysis and parameter estimation. The astrophysical significance of studying precessing systems is also discussed. In chapter 2 we introduce the concept of 'matching' as a method for quantifying the degenerecy between different waveforms with minimal computational effort, and use these matches to identify the parts of the parameter space that would be most fruitful to explore. In chapter 3 we describe the process of software injections, where simulated signals are inserted into detector noise and then recovered using the inference methods introducted in the introduction. This gives a way of probing the detector response to a given signal. We present results from a range of software injections guided by the match findings, and attempt to analyse how effectively the current infrastructure is capable of inferring spin parameters on precessing BBHs. Finally we briefly consider the impact of the upcoming VIRGO detector on spin inference.

1.2 Gravitational waves and their sources

A complete analysis is available in Hartle[12], but here we briefly overview the fundamental theory of gravitational waves. In the general theory of relativity, gravity is a consequence of the curvature of a 4-dimensional spacetime as described by the Einstein equation (in natural units):

$$R_{\alpha\beta} - \frac{1}{2} g_{\alpha\beta} R = 8\pi T_{\alpha\beta} \tag{1}$$

where $R_{\alpha\beta}$ is the Riemannian curvature tensor, $g_{\alpha\beta}$ is the metric tensor, R is the Ricci scalar and $T_{\alpha\beta}$ is the energy-momentum tensor. This equation is essentially ten non-linear partial differential equations, where we use the Einstein summation convention to sum over all indices, and where indices run from 0 to 4. Intuitively, the LHS of this equation can be thought of as the local curvature of spacetime, and the RHS quantifies the energy and momentum density. In the weak-field regime, where the curvature of spacetime is low, the metric tensor can be approximated as

$$g_{\alpha\beta}(x) = \eta_{\alpha\beta} + h_{\alpha\beta}(x). \tag{2}$$

where $\eta_{\alpha\beta}$ is the Minkowski metric and $|h_{\alpha\beta}| \ll 1$ for all components. This metric can be substituted into the Einstein equation, and expanding in $h_{\alpha\beta}$ in first order and using the Lorentz gauage, the Einstein equation becomes

$$\Box h_{\alpha\beta} = 0 \tag{3}$$

where $\Box$ is the D'Alembertian operator, with

$$\partial_\beta h^\beta_\alpha - \frac{1}{2} \partial_\alpha h^\beta_\beta = 0. \tag{4}$$

The general solution to this equation is

$$h_{\alpha\beta} = \begin{pmatrix} 0 & 0 & 0 & 0 \\ 0 & a_+ & a_\times & 0 \\ 0 & a_\times & -a_+ & 0 \\ 0 & 0 & 0 & 0 \end{pmatrix} e^{i\omega(z-t)} \tag{5}$$

for a wave with frequency ω propagating in the z direction. Here the a_+ and $a_\times$ terms represent the amplitudes of the 'plus' and 'cross' polarisations respectively. As a gravitational wave passes through an observer, spacetime is distorted along the spatial directions orthogonal to the propagation direction of the wave according to these polarisation amplitudes. A visualisation of this is

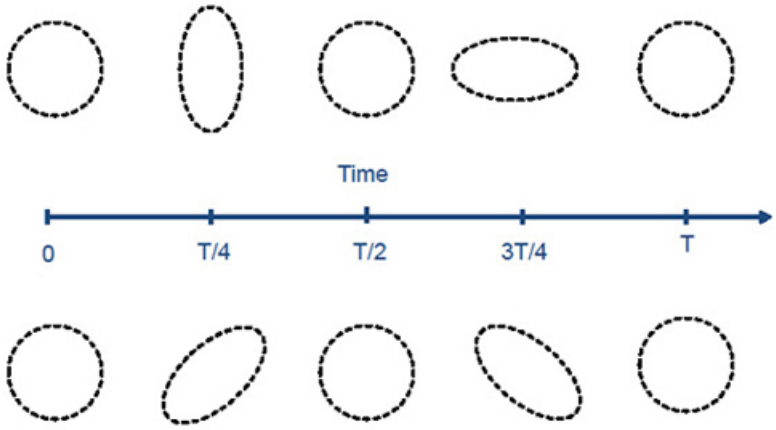

Figure 1: [13]Plus and cross polarisations respectively of a gravitational wave propagating through the page, with scale greatly exagerrated.

shown in Fig. 1. It is this stretching and squeezing of spacetime that the LIGO detectors were built to detect.

Now we consider the sources of these waves. Analysis in this area can rapidly become extremely complicated as the weak-field approximation is dropped and higher orders of perturbations are included[14], but the simplest case is still instructive.

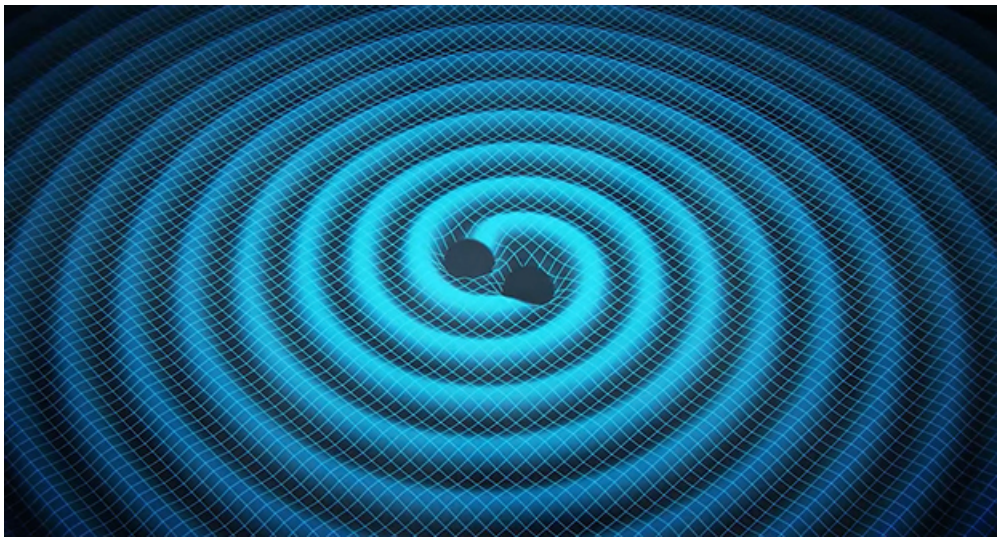

Figure 2: [15]Impression of two inspiralling compact objects emitting gravitational waves

Approximating that the field around the source is still weak, that the wavelength is long and that the observer is a large distance from the source, the spatial elements of the GW metric are

$$h_{ij} \approx \frac{2}{r}\ddot{I}^{ij}(t-r) \tag{6}$$

where I^{ij} is the second mass moment given by

$$I^{ij}(t) = \int d^3x \mu(t,\vec{x}) x^j x^j \tag{7}$$

where $\mu(t, \vec{x})$ is the mass density of the system. The energy loss of a binary system emitting gravitational waves is

$$L_{GW} = \frac{128}{5} M^2 R^4 \Omega^6, \tag{8}$$

and as the binary loses energy, the separation between the compact objects decreases, increasing the orbital frequency. Given the connection between the mass distribution of the system in (7) and the GW amplitudes in (6), this gives rise to a 'chirp' effect seen in the signal of a CBC GW. This is shown in a Fig. 3. which is a simulated waveform of the merging of a BBH system.

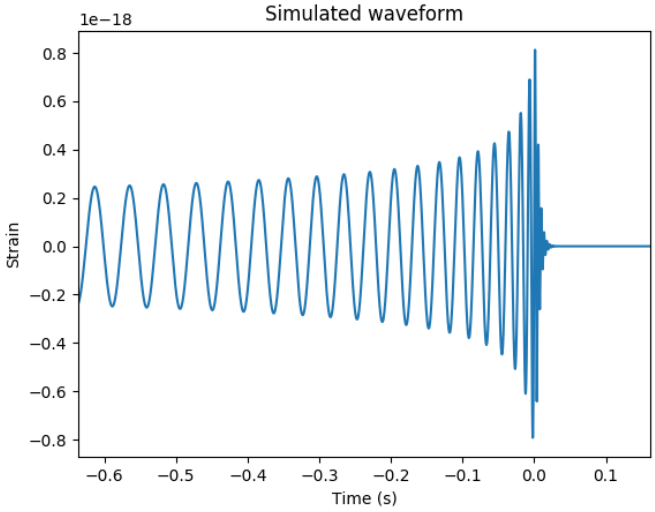

Figure 3: Simulated waveform of a BBH merger of two 35 solar mass black holes.

The waveform can be split into three phases - the inspiral, the merger and the ringdown. The frequency, frequency evolution and amplitudes of each polarisation of the GW emitted from a merger will depend on the properties of the system itself, and as such there is information about the source contained in the specific morphology of a GW signal.

1.3 LIGO

The fundamental physical principle of the LIGO detectors is that they are laser interferometeres. Interferometers are devices that can measure changes in length to extremely high accuracy using constructive and destructive interference, as shown in Fig. 4. Light leaves the laser beam, and is split down the two arms of the detector by the beam splitter. If the length of the two arms is equal, the optical path difference between the two light beams is zero, and the two beams constructively interfere after recombining at the beam splitter. However if there is any change in the length of one of the arms, the beams will no longer constructively interfere and the photodetector will register a change in intensity. As a gravitational wave passes through the detector, the relative length of the arms changes, and the GW signal is recorded by the photodiode. A large part of the scientific and engineering effort at LIGO involves techniques to minimise and account for noise in the system, and the recent advanced LIGO upgrade to the detectors increased the effective volume within which mergers can be detected by a factor of 3[17][18]. Some of these techniques include suspending the mirrors from a series of pulleys and penduli, and applying real time corrections to the positions of the mirrors to compensate for external seismic noise. There is also considerable effort in managing the optics and lasers of the system in order to maximise the coherence of the laser beam and the intensity detected in the photodiode[19]. The noise spectrum for advanced LIGO is shown in Fig. 5.[16], where the sharp noise peaks are specifically designed resonances that are extracted out of

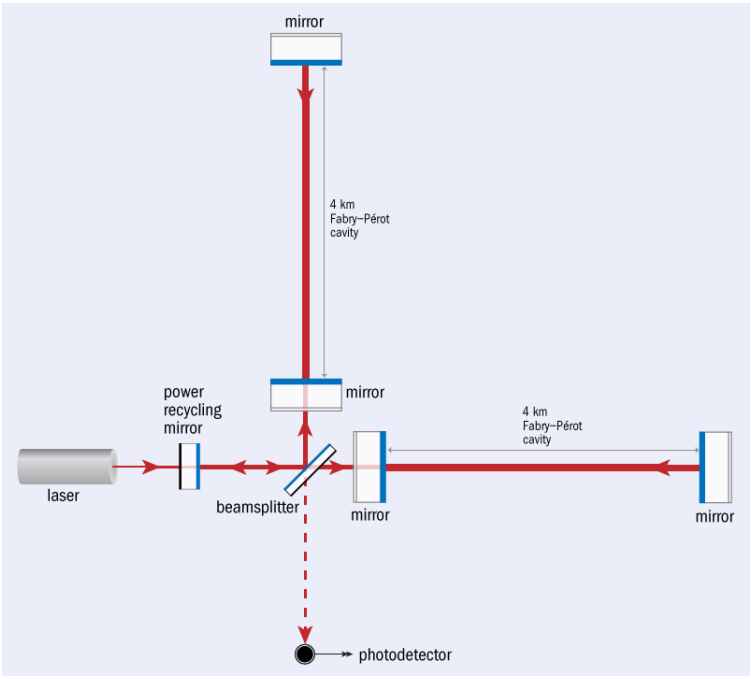

Figure 4: Simplified schematic of a LIGO detector http://images.iop.org/objects/phw/news/20/2/10/ligo-figure.png

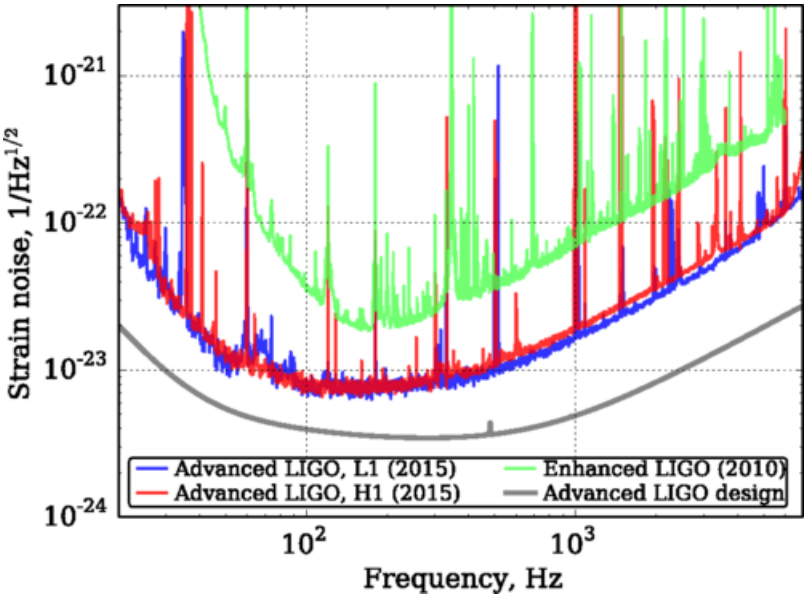

Figure 5: [16]Noise spectrum for advanced LIGO detectors.

the strain data. The strain data observed in the detector is a function of the different polarisation amplitudes

$$h(t) = F^{+}(\alpha, \delta, \psi)h_{+}(t) + F^{\times}(\alpha, \delta, \psi)h_{\times}(t), \tag{9}$$

where $F^{+}(\alpha, \delta, \psi)$ and $F^{x}(\alpha, \delta, \psi)$ are the antenna beam patterns that describe how the detector responds to signals at different sky locations and polarisations[20]. In first order, the polarisations are given by

$$h_{+}(t) = A_{GW}(t)(1 + cos^{2}(\iota)cos(\phi(t))) \tag{10}$$

$$h_{\times}(t) = -2A_{GW}(t)cos(\iota)sin(\phi(t)) \tag{11}$$

and binaries that are face on (with $\iota = 0$) emit circularly polarised waves, and edge-on binaries emit linearly (either cross or plus) polarised GWs.

1.4 Parameter estimation and Bayesian inference

A signal is described by a total of 16 parameters[21] - time and phase of coalesence t_c and ϕ_c, two parameters to describe sky location (right ascension, α and declination δ), distance d, inclination angle ι describing the orientation of the binary's total angular momentum with respect to the line of sight, polarisation angle ψ, the masses m_1, m_2, six spin parameters to totally describe the spins on each of the two black holes $\vec{S}_1$, $\vec{S}_2$, and then two eccentricity parameters.

1.5 MCMC

Overview of MCMCs that will be used for inference

1.6 Precession

Precessing binaries and effective spin parameters

1.7 Astrophysical implications

Binary formation models and how estimating chi p is significant for distinguishing bewteen them

2 Matching

Describe matching, and how matches are used to run targeted software injections. Then identify parameter combinations where we are particularly sensitive to chi p, and those where we are not

3 Software injections

Describe software injections

3.1 Signal extraction

Data whitening - basically LOSC stuff, how we go from raw data to a signal - move this to intro?

3.2 Inference pipeline

Describe the structure of the inference pipeline

3.3 Inference runs

Posteriors and discussion of inference results

3.4 Impact of Virgo

A look at how Virgo will influence PE, especially chi p estimation

4 Conclusions and implications

Summary of results on PE and estimation of chi p, and a prospect on Virgo's impact.

References

[1] B. P. Abbott et. al. Observation of gravitational waves from a binary black hole merger. *Physical Review Letters*, 116(6), Feb 2016.

[2] B. P. Abbott et. al. GW151226: Observation of gravitational waves from a 22-solar-mass binary black hole coalescence. *Physical Review Letters*, 116(24), Jun 2016.

[3] A. Einstein. Nherungsweise integration der feldgleichungen der gravitation. *Sitzungsberichte der Kniglich Preussischen Akademie der Wissenschaften Berlin*, (688-696), 1916.

[4] A. Einstein. ber gravitationswellen. *Sitzungsberichte der Kniglich Preussischen Akademie der Wissenschaften Berlin*, (154-167), 1918.

[5] W. Steinicke. Einstein and the gravitational waves. *Astronomische Nachrichten*, 326(7), 2005.

[6] N. Rosen A. Einstein. On gravitational waves. *Journal of the Franklin Institute*, 223(43-54), 1937.

[7] J. H. Taylor and J. M. Weisberg. A new test of general relativity - gravitational radiation and the binary pulsar PSR 191316. *The Astrophysical Journal*, 253:908, Feb 1982.

[8] Marica Branchesi. Multi-messenger astronomy: gravitational waves, neutrinos, photons, and cosmic rays. *Journal of Physics: Conference Series*, 718:022004, May 2016.

[9] B. P. Abbott et. al. Prospects for observing and localizing gravitational-wave transients with advanced ligo and advanced virgo. *Living Reviews in Relativity*, 1:19, Dec 2016.

[10] Xavier Calmet, Iberê Kuntz, and Sonali Mohapatra. Gravitational waves in effective quantum gravity. *The European Physical Journal C*, 76(8), Jul 2016.

[11] Pau Amaro-Seoane et al. Low-frequency gravitational-wave science with eLISA/NGO. *Classical and Quantum Gravity*, 29(12):124016, Jun 2012.

[12] James B. Hartle. *Gravity: An Introduction to Einstein's General Relativity*. Addison Wesley, 2003.

[13] Unknown. Accessed 09/04/2017.

[14] Luc Blanchet, Thibault Damour, Bala R. Iyer, Clifford M. Will, and Alan G. Wiseman. Gravitational-radiation damping of compact binary systems to second post-newtonian order. *Physical Review Letters*, 74(18):3515–3518, May 1995.

[15] Swinburne Astronomy Productions. Accessed 09/04/2017.

[16] D. V. et al. Martynov. Sensitivity of the advanced ligo detectors at the beginning of gravitational wave astronomy. *Phys. Rev. D*, 93:112004, Jun 2016.

[17] D. V. Martynov et al. Sensitivity of the advanced LIGO detectors at the beginning of gravitational wave astronomy. *Physical Review D*, 93(11), Jun 2016.

[18] J. et al. Abadie. Sensitivity Achieved by the LIGO and Virgo Gravitational Wave Detectors during LIGO's Sixth and Virgo's Second and Third Science Runs. 2012.

[19] J Aasi et al. Advanced LIGO. *Classical and Quantum Gravity*, 32(7):074001, Mar 2015.

[20] Robert L. Forward. Wideband laser-interferometer graviational-radiation experiment. *Phys. Rev. D*, 17:379–390, Jan 1978.

[21] B. P. Abbott et al. Properties of the binary black hole merger GW150914. *Physical Review Letters*, 116(24), Jun 2016.